Kicked-rotor quantum resonances in position space: Application to systems of experimental interest

Maxence Lepers ‡, Véronique Zehnlé and Jean-Claude Garreau

Laboratoire de Physique des Lasers, Atomes et Molcules, Universit Lille 1 Sciences et Technologies, CNRS; CERLA; F-59655 Villeneuve d'Ascq Cedex, France

Abstract. In a previous article [1], we have presented an original approach of the quantum resonances of the kicked rotor. We have described the quantum resonances in position space, for strongly localized wave packets in comparison to one step of the kicking potential. In the present article, we extend that approach to experimentally accessible systems, characterized, on the contrary, by delocalized wave functions in position space. We demonstrate that the intuitive picture developed previously is still applicable here. As examples, we consider the dynamics of a thermal gas and of a Bose-Einstein condensate, both for simple and high-order quantum resonances. Our numerical simulations enable us to predict new interesting phenomena, that are explained in a large extent by analytical calculations.

PACS numbers:

1. Introduction

Over the last 30 years, the *kicked rotor* has played a central role in the field of "quantum chaos", defined as the study of quantum systems whose classical counterpart is chaotic [2, 3, 4]. With the advent of its first experimental realization in 1995 [5], obtained by submiting laser-cooled atoms to a periodic series of kicks of a laser standing wave, an impressive number of experimental results followed [6, 7, 8, 9, 10, 11, 12, 13, 14], spreading to domains like quantum transport [15], measurements of the gravitational constant [16], and even condensed matter and quantum phase transitions with, recently, the first experimental observation of the metal-insulator Anderson transition with matter waves [14, 17, 18].

One of the most striking features of the QKR is the existence, of *quantum resonances* (QRs), which arise if the kicking period matches the evolution of the quantum phase of the atom. A QR is characterized by a *ballistic* behavior, in which the velocity increases linearly, and the kinetic energy increases quadratically. QRs in the kicked rotor and in the kicked accelerator (in which the atoms are also submitted to a constant force) have been observed both with laser-cooled gases and Bose-Einstein

‡ Present address: Laboratoire Aimé Cotton, Université Paris-Sud, Bat. 505, Campus d'Orsay, F-91405 Orsay Cedex, France

condensates (BECs), leading to impressive amount of theoretical and experimental studies [8, 19, 20, 21, 22, 23, 24, 25].

The atomic kicked rotor is obtained by placing laser-cooled atoms of mass M and momentum p in a standing wave formed by counterpropagating (along the x-axis) laser beams of intensity I_L, wave number $k_L = 2\pi/\lambda_L$ and detuning Δ_L. The atom is submitted to a conservative dipole force, associated to an "optical potential" $V(x) \propto (I_L/\Delta_L)\sin^2(2k_L x)$. If the standing wave is modulated in the form of pulses of duration τ very short at the timescale of the dynamics§, one obtains the kicked-rotor Hamiltonian

$$H = \frac{P^2}{2} + K\cos X \sum_n \delta(t-n), \tag{1}$$

where we introduced reduced variables [5] in which time is measured in units of the kick period T, $X = 2k_L x$, $P = \hbar p/2\hbar k_L$, $K = \hbar I_L \Gamma^2 \tau/8 I_s \Delta_L$, where I_s is the saturation intensity of the atomic transition and $\hbar = 4\hbar k_L^2 T/M$ plays the role of a reduced Planck's constant ‖.

The spatial periodicity $\lambda_L/2$ of the standing wave implies that the quasimomentum β, defined by the relation

$$P = (n+\beta)\,\hbar, \tag{2}$$

where n is an integer and $\beta \in [-\frac{1}{2}; \frac{1}{2})$, is a constant of motion. In position space, the wave function corresponding to a particular quasimomentum $\psi_\beta(X)$ has the well-known Bloch-wave structure

$$\psi_\beta(X) = e^{i\beta X} u_\beta(X), \tag{3}$$

where $u_\beta(X)$ has the same spatial period 2π as the standing wave¶. In a previous paper [1], we introduced an original approach of QRs, based on the study of localized wave functions $u_\beta(X)$. We developed an intuitive interpretation of the QRs, based on an analogy between the quantum resonances and the classical accelerator modes of the kicked rotor [4]. The spatial invariance of the potential under translations by a multiple of its periodicity allows us to "fold" the position space into a finite interval $X \in [-\pi, \pi)$ (as usual in kicked-rotor studies). In this context, saying that the packet is "localized" in position space means that actually it forms a comb in position space, with indentical packets separated by 2π.

When a comb-shaped wavepacket propagates freely it *resumes its initial shape* if the propagation time is a rational multiple of a characteristic time, called the Talbot time, in analogy to the optical Talbot effect [26],

$$T_T = \frac{\pi M}{\hbar k_L^2}, \tag{4}$$

§ That is $p\tau/M \ll \lambda_L$ for all values of the atomic momentum p.

‖ In the sense that the Schrdigner equations reads $i\hbar\partial\psi/\partial t = H\psi$.

¶ The atom wave function is $\psi(X) = \int_{-1/2}^{1/2} d\beta \psi_\beta(X)$.

(correponding to $\hbar = 4\pi$ in reduced units). This is the Talbot effect. If the interval between kicks is commensurable with the Talbot time (that is, if $\hbar$ is comensurable with 4π), the kicks are applied to a wavepacket that *has always the same form*, which leads to a *coherent adding* of the kick effect [1]. In consequence, each kick transfers the same amount of momentum to the atom, which thus increases linearly.

Consider now the one-period evolution operator for the quantum kicked rotor

$$U = \exp\left(-i\frac{K}{\hbar}\cos X\right)\exp\left(-i\frac{P^2}{2\hbar}\right), \tag{5}$$

where factorization is allowed because the kicks are instantaneous. The parameter $\hbar$ can be experimentally tuned by changing the kicking period T, determining the appearance of quantum resonances. In section 2 we show that if $\hbar = 2\pi\ell$ with ℓ integer, the initial wavepacket perfectly reconstructs itself at the end of a free evolution between kicks, giving rise to the so-called *simple quantum resonances* (SQRs). By contrast, if $\hbar = 4\pi r/s$, with r, s integers and $s > 2$, the initial wavepacket reconstructs in at least two sub-packets, giving the so-called *high-order quantum resonances* (HOQRs). Ref. [1] mention that the simple image given above cannot be directly applied to high-order quantum resonances, because the two subpackets produce additional interference effects. In section 3 we consider the $\hbar = \pi$ case, and we extend our previous results to the calculation of the mean kinetic enegy, and give analytical expressions in the $\beta = 0$ case.

Once again, it is important to stress that the interpretation of QRs introduced in Ref. [1] was based on *localized wave functions in position space*. By contrast, the dynamical behaviors associated with QRs have been observed with Bose gases, where the initial state is close to a plane wave. In the present paper, we show that the ideas developed in [1] can be applied to explain the dynamics in experimentally accessible situations. This is due to the fact that the localized wave functions play the role of quasi-eigenstates of the system [27], on which any other state can be expanded. We shall consider two limits: an initial momentum distribution much narrower than the first Brillouin zone, corresponding to a Bose-Einstein condensate, and the opposite limit of an incoherent initial momentum distribution much larger than the first Brillouin zone, corresponding to thermal clouds, where all quasimomenta are more or less equally populated. In this way, we render our results applicable to a wide variety of situations of experimental interest.

2. Simple quantum resonances

"Simple" quantum resonances are the quantum-mechanical analog of the half-Talbot effect in optics, in which the propagation time is a multiple of the Talbot time. In the KR scaled units, a simple quantum resonance takes place when $\hbar = 2\pi\ell$ for an integer valuer ℓ. In this section, we recall the results of ref. [1] for a state of well-defined quasimomentum, and then apply these ideas to an initial state composed of

several quasimomenta. All our interpretations are based on the quantum-resonance map derived for mean position and momentum of the atom [1].

2.1. Well-defined quasimomentum

Given a state $\psi_\beta(X,t)$ of well-defined quasimomentum β, one can use the one-period evolution operator Eq. (5) to relate it to the wave function $\psi_\beta(X,t+1)$ one period later. In the case of a SQR this produces a simple recursion relation which has a particularly simple form [see [1], Eq. (10)]:

$$\psi_\beta(X,t) = e^{-i\kappa\cos X}\exp\left(i\hbar\beta(\beta+1)/2\right)\psi_\beta\left(X-\hbar\left(\beta+1/2\right),t-1\right) \tag{6}$$

where κ is related to the kick amplitude

$$\kappa \equiv K/\hbar. \tag{7}$$

The term $\exp\left(i\hbar\beta(\beta+1)/2\right)$ in Eq. (6) is a global phase that does not influence the wavepacket dynamics.

The free evolution between kicks preserves the shape of ψ_β but translates over the distance v given by the "velocity"

$$v = \hbar\left(\beta+\frac{1}{2}\right), \tag{8}$$

The average position of the wavepacket $\langle X\rangle_\beta$ obeys the recursion relation

$$\langle X\rangle_\beta(t) = \langle X\rangle_\beta(t-1) + v\,. \tag{9}$$

The application of the kick operator changes the average momentum as

$$\langle P\rangle_\beta(t) = \langle P\rangle_\beta(t-1) + K\int_{-\pi}^{\pi} dX\sin(X+vt)\left|\psi_\beta(X,t=0)\right|^2 \tag{10}$$

and the average kinetic energy as

$$\begin{aligned}\langle E\rangle_\beta(t) = \langle E\rangle_\beta(t-1) &+ \frac{K^2}{2}\int_{-\pi}^{\pi} dX\sin^2(X+vt)\left|\psi_\beta(X,0)\right|^2 \\ &+ K\int_{-\pi}^{\pi} dX\sin(X+v)J(X,t-1),\end{aligned} \tag{11}$$

where we introduced the current

$$J(X,t) = i\frac{\hbar}{2}\left(\psi_\beta(X,t)\partial_X\psi^*_\beta(X,t) - c.c.\right). \tag{12}$$

If we consider initially a Bloch wave perfectly localized at X_0 [+],

$$\psi_\beta(X,t=0) = e^{i\beta X}\sum_j \delta\left(X - X_0 - 2\pi j\right), \tag{13}$$

Eq. (10) yields for the average momentum:

$$\langle P\rangle_\beta(t) = \langle P\rangle_\beta(t-1) + K\sin(X_0+vt). \tag{14}$$

[+] Let us stress again that here "localized" means localized in the "spatial" first Brillouin zone $[-\pi,\pi)$, the full wave function is a comb of delta functions. In the momentum space the wavefunction is also a Dirac comb, thus satisfying Heisenberg's principle.

Noting that

$$\int_{-\pi}^{\pi} dX\, J(X,t) = \langle P \rangle_\beta (t), \tag{15}$$

we get for the average kinetic energy

$$\langle E \rangle_\beta (t) = \langle E \rangle_\beta (t-1) + \frac{1}{2} K^2 \sin^2(X_0+vt) + K \sin(X_0+vt) \langle P \rangle_\beta (t-1). \tag{16}$$

A consequence of Eqs. (14) and (16) is that

$$\langle E \rangle_\beta (t) - \langle E \rangle_\beta (t-1) = \frac{1}{2} \left(\langle P \rangle_\beta^2 (t) - \langle P \rangle_\beta^2 (t-1) \right),$$

thus the average kinetic energy $\langle E \rangle_\beta$ and the average square momentum $\langle P \rangle_\beta^2 /2$ have the same dynamical evolution, which is characteristic of a classical particle. The evolution of these observables can thus be written as a classical-like map

$$X_\beta(t) = X_\beta(t-1) + v = X_0 + vt \tag{17}$$

$$\begin{aligned} P_\beta(t) &= P_\beta(t-1) + K \sin(X_0 + vt) \\ &= P_\beta(0) + K \sum_{s=1}^{t} \sin(X_0 + vs), \end{aligned} \tag{18}$$

where we have set $X_\beta(0) = X_0$, $P_\beta(t) = \langle P \rangle_\beta (t)$. Also

$$E_\beta(t) - E_\beta(0) = \frac{1}{2} \left(P_\beta^2(t) - P_\beta^2(0) \right). \tag{19}$$

To calculate the observables *dynamics*, one has simply to average Eqs. (17) and (18) over the *initial* distribution.

2.2. Average over the quasimomentum

Let us now discuss the situation where the initial momentum distribution contains different quasi-momenta. We shall consider two extreme examples of what is experimentally feasable: an initial momentum distribution much narrower than the Brillouin zone, and a much wider one, for which all quasimomentum classes are equally populated.

2.2.1. Narrow initial momentum distribution. Consider an initial momentum distribution localized around $P = 0$ of width $\hbar\Delta$, with $\Delta \ll 1$. This is e.g. the case for Bose-Einstein condensates ($\Delta \sim 10^{-3} - 10^{-2}$). We can expect the behavior of such a system to be dominated by the central momentum, but additional effects due to the finite width arise.

We start with the case $\beta = 0$, where only the $n = 0$ component is initially populated, i.e. a plane wave. As all values of X are equiprobable, the integration of Eq. (18) gives

$$\begin{aligned} P_0(t) &= P_0(0) + K \int_{-\pi}^{\pi} dX_0 \sum_{s=1}^{t} \sin(X_0 + vs) \\ &= P_0(0) = 0. \end{aligned} \tag{20}$$

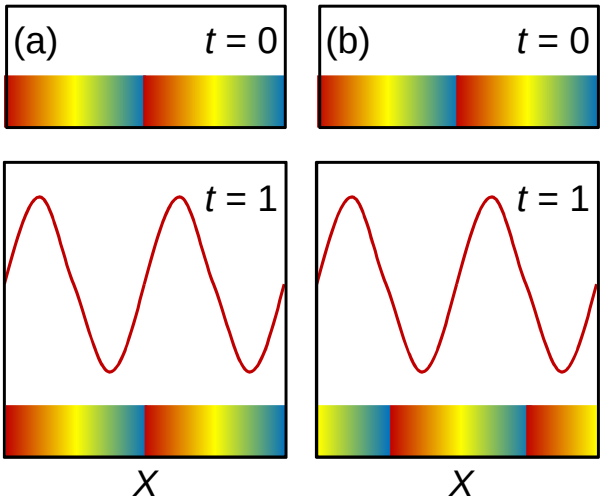

Figure 1. (color online) Dynamics of a plane wave: (a) In the ballistic case $\hbar = 4\pi$, and (b) in the periodic one $\hbar = 2\pi$. The initial distribution, uniform is position space (restricted here to two potential wells), is "sliced" with different colors. At the first kick, panel (a), each slice, after its free evolution has come back to the initial position and thus receives the same momentum from the kick. On panel (b), each color is shifted by half the lattice step, and thus receives a kick of the same magnitude as in (a), but of opposite direction.

From Eq. (19), the kinetic energy is

$$E_0(t) - E_0(0) = \frac{K^2}{2} \int_{-\pi}^{\pi} dX_0 \left(\sum_{s=1}^{t} \sin(X_0 + vs) \right)^2 = \frac{K^2}{4} \frac{\sin^2(vt/2)}{\sin^2(v/2)}, \tag{21}$$

which is the result of Ref. [23]. If $v = 0[2\pi]$, where $[2\pi]$ means "modulo 2π", (e.g. $\hbar = 4\pi$) the dynamics is ballistic: $E_\beta(t) = E_\beta(0) + K^2 t^2/4$, whereas if $v = \pi[2\pi]$ (e.g. $\hbar = 2\pi$) the dynamics is periodic (or "anti-resonnant"), i.e. $E_\beta(t) = E_\beta(0) + K^2/4$ for t odd and $E_\beta(t) = E_\beta(0)$ for t even.

Figure 1 gives a simple interpretation of these behaviors that bears a striking relationship with the mecanism of classical accelerator modes of the kicked rotor [28]. On both panels (a) and (b), the initial probability distribution is uniform, but we have attributed a different color at each slice of it so that one can follow its evolution. Eq. (17) shows that the evolution results in a simple global shift of the wave function between $t = 0$ and $t = 1$ kick. In the ballistic case (a), this shift is such that all "colors" (or slices) come back at the same place at $t = 1$ (and also at $t = 2, 3, ...$), so that, each part of the wave function receive the same kick (for example the yellow part receives the maximum momentum transfer $+K$). As the wave function fills uniformly in the potential wells when the kicks are applied, the average momentum is always zero, but the average kinetic energy grows quadraticlly, since some "colors" are accelerated in the positive direction, while others are accelerated in the negative direction.

By contrast, figure 1 (b) illustrates the so-called anti-resonant case, for which the

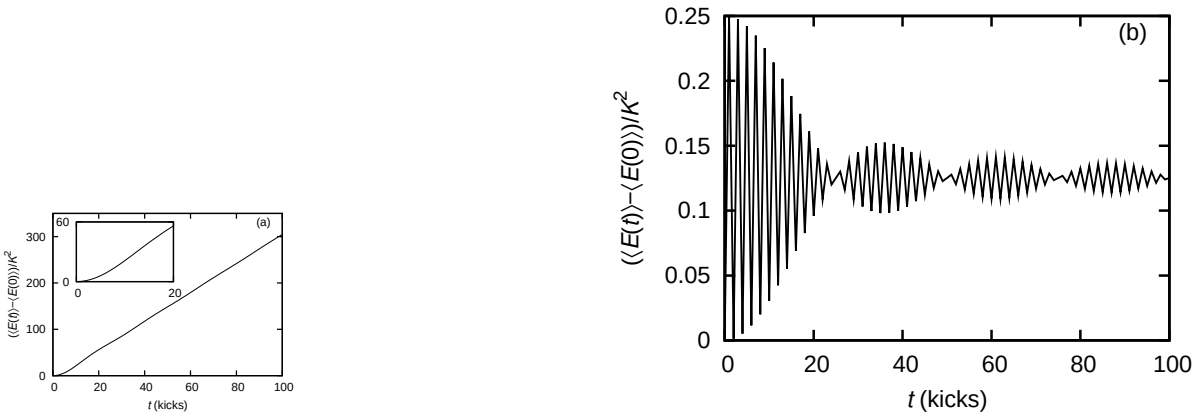

Figure 2. Time evolution of the mean kinetic energy for a narrow initial momentum distribution ($\Delta = 0.04$). On panel (a), for which $\hbar = 4\pi$, the central quasi-momentum is ballistic, whereas it is anti-resonant on panel (b), for which $\hbar = 2\pi$. These plots, like all plots of the mean kinetic energy in this article, were obtained by direct application of Eq. (5).

wavepacket is shifted half of the lattice step. At odd values of t, a given "color" receives a momentum equal to $-K \sin X_0$, whereas at even values of t, it receives $+K \sin X_0$, hence a periodic behavior.

Let us now consider the case of a narrow initial momentum distribution centered at $P = 0$, $\rho(\beta) = 1/\Delta$ for $|\beta| \leq \Delta/2$ and zero otherwise, with a width $\hbar\Delta \ll 1$. Figure 2 shows the time evolution of the average kinetic energy, for momentum distributions whose central component exhibits ballistic (a) and anti-resonant (b) dynamics. Those characteristic behaviors are clearly visible in the early dynamics, but they are progressively damped due to the finite width of the distribution. Averaging Eq. (2) over the initial quasimomentum distribution:

$$\begin{aligned} E(t) &= \frac{1}{\Delta}\int_{-\Delta/2}^{\Delta/2} d\beta E_\beta(t) \\ &= \quad E(0) + \frac{K^2}{4\Delta}\int d\beta \frac{\sin^2\left(\pi\ell\left(\beta+1/2\right)t\right)}{\sin^2\left(\pi\ell\left(\beta+1/2\right)\right)}, \end{aligned} \tag{22}$$

shows a diffractive filtering of quasimomentum, which becomes more and more selective as time increases. The damping process is significant after a characteristic time $\tau_d \sim \Delta^{-1}$, such that the first zero of the filtering function coincides with the edge of the initial momentum distribution. For $t \gg \tau_d$, the behavior associated with the central momentum is completely damped.

We see in Fig. 2(a) that the quadratic increase of the kinetic energy quickly turns into the usual linear one, but with a different diffusion rate. To explain this result, we consider the case $\hbar = 4\pi$, $\beta \approx 0$, and approximate the filtering function in Eq (21), for $\beta t \leq 1$ by

$$\frac{\sin^2(2\pi\beta t)}{\sin^2(2\pi\beta)} \approx t^2 \cos^2\left(\pi\beta t\right). \tag{23}$$

If $t \leq 1/\Delta$, the initial momentum distribution is "totally included" in the central lobe; therefore the mean kinetic energy reads

$$\begin{aligned} E(t) &= \frac{1}{\Delta}\int_{-\Delta/2}^{\Delta/2} d\beta E_\beta(t) \\ &\approx E(0) + \frac{K^2t^2}{4\Delta}\int_{-\Delta/2}^{\Delta/2} d\beta \cos^2(\pi\beta t) \\ &\approx E(0) + \frac{K^2t^2}{8}\left(1 + \frac{\sin(\pi\Delta t)}{\pi\Delta t}\right). \end{aligned} \tag{24}$$

As expected, Eq. (24) shows that the early dynamics (i.e. for $t \ll \Delta^{-1}$) is ballistic, with a rate equal to $K^4/4$. Then, as t approaches $1/\Delta$, Eq. (24) suggests that the dynamics remains ballistic, but that the rate decreases progressively from $K^2/4$ to $K^2/8$. However, Eq. (24) fails to acount for the progressive appearance of the linear contribution to the mean kinetic energy. This is because the approximation of the filtering function (see Eq. (23)) becomes less accurate as t approaches Δ^{-1}.

For $t > \Delta^{-1}$, the edges of $\rho(\beta)$ are located out of the central lobe of the filtering function. To highlight the essential features of the dynamics, we separate in the integral of Eq. (22) the contribution of the central lobe of the filtering function from that of the other lobes. As the central lobe gets thinner as times goes by, the bonds of the integral due to the central lobe are time-dependent. Namely, Eq. (22) reads

$$\begin{aligned} E(t) \approx E(0) &+ \frac{K^2t^2}{4\Delta}\int_{-1/2t}^{1/2t} d\beta \cos^2(\pi\beta t) \\ &+ \frac{K^2}{2\Delta}\int_{1/2t}^{\Delta/2} d\beta f(\beta, t), \end{aligned} \tag{25}$$

where $f(\beta, t)$ is the function that approximates all lobes expect the central one, defined for $1 \leq \beta t$. The term on the last line of (25) only generates oscillations of the energy. By contrast, the first line of (25) yields a diffusive behavior

$$E(t) \approx E(0) + \frac{K^2 t}{8\Delta}, \tag{26}$$

whose rate, with the parameters of Fig. 2 (a), is equal to 312.5. This analytical rate is in very good agreement with the one obtained from a linear fit of the curve from $t = 25$ to 200 kicks, which is 312.4.

In the anti-resonant case on Fig. 2 (b), the energy, although damped, oscillates for a time equal to a few Δ^{-1}, and finally "freezes" at $K^2/8$. To catch the most important features of the dynamics, we will once again take an approximate form for Eq. (22). Indeed, we consider that the term $\sin^2\{\pi\ell(\beta + 1/2)\}$ evolves so slowly on the scale of Δ, that it can be taken as unity. By expanding $\sin^2\{\pi\ell t(\beta + 1/2)\}$, one gets

$$E(t) \approx E(0) + \frac{K^2}{8}\left[1 - \frac{1}{\Delta}\int_{-\Delta/2}^{\Delta/2} d\beta \cos\{2\pi t(\beta + 1/2)\}\right], \tag{27}$$

where $E(0) = \hbar^2\Delta^2/24$. Thus

$$E(t) \approx \frac{\hbar^2\Delta^2}{24} + \frac{K^2}{8}\left[1 - (-1)^t \frac{\sin(\pi\Delta t)}{\pi\Delta t}\right]. \tag{28}$$

For $t \gg \Delta^{-1}$ the oscillations are completely damped and the energy tends to its asymptotic value

$$E(t \to \infty) = E(0) + \frac{K^2}{8}. \tag{29}$$

Incidentally, if one keeps in Eq. (27) a general momentum ditribution $\rho(\beta)$ the equation shows that the kinetic energy is proportional to the cosine-Fourier series of the momentum distribution. Using the properties of Fourier series, we can "invert" Eq. (27) to

$$\rho_t(\beta) = \sum_{s=1}^{t} \frac{4}{K^2} \left(E(0) - E(t)\right) \cos\left(2\pi t \left(\beta + \frac{1}{2}\right)\right), \tag{30}$$

which yields an approximate analytical formula for the initial momentum distribution. Eq. (30) suggests that, by measuring the mean kinetic energy of an atomic cloud submitted to a series of pulses, one can obtain an analytical approximation for the momentum distribution of the cloud. Since it appears as a Fourier series, the accuracy of this approximation increases with the measurement time, i.e. $\rho_t(\beta) \to \rho(\beta)$ when $t \to \infty$. Moreover, the resolution in momentum gets also betteer with time, as it is equal to $1/t$. This result is valid for narrow momentum distributions that contain no ballistic quasi-momentum. As ballistic quasi-momenta get more numerous as $\hbar$ increases, the phenomenon is more likely to be observed for $\hbar = 2\pi$.

2.2.2. "Broad" initial momentum distribution. For the sake of completenes, we consider now the relatively trivial case of an initial momentum distribution that is a few times larger than the Brillouin zone. This cases leads to a well-known diffusive behavior, which can be demonstrated by taking the average on X and of β of Eq. (21). If one considers a slice centered at position X containing all quasi-momenta, Eq. (17) shows that after one kick the slice corresponding to quasimomentum β moves to $X + 2\pi\ell\,(\beta + 1/2)$, which means that it covers a whole potential well. Therefore, the avearge momentum does not change, and the kinetic energy is increased by $K^2 \left\langle \sin^2 \right\rangle_\beta /2 = K^2/4$; averaging over X does not change the result. As the same situation reproduces at each kick the effect on the kinetic energy is additive:

$$E(t) = E(0) + \frac{K^2}{4} t. \tag{31}$$

It is worth noting that the equiprobability of all positions X of a classical ensemble of particles can also be used to explain the classical ergodic for high enough K, this result is thus a classical one, averging over quasimomentum erases the quantum character of the process.

3. The $\hbar = \pi$ high-order quantum resonance

A higher-order quantum resonance (HOQR) is the analog of the fractional Talbot effect. The $\hbar = \pi$ resonance corresponds to a situation where the initial wave packet

reconstructs into two "sub-packets. In ref. [1], it was shown that the two "sub-packets" mimick a two-level system. The present section extends this approach in order to allow an analytical calculation of the average kinetic energy.

3.1. Recursion relation and average momentum

In Ref. [1], we found a recursion relation for the wave function at integer times t

$$\psi_\beta(X+wt,t) = \frac{e^{-i\kappa\phi(X,t)}}{\sqrt{2}}\Big[e^{-i\pi/4}\psi_\beta\left(X+w(t-1),t-1\right) + e^{i\pi/4}e^{i\beta\pi}\psi_\beta\left(X+w(t-1)-\pi,t-1\right)\Big], \tag{32}$$

where $w = \hbar\beta$ and $\phi(x,t) = \kappa\cos(X+wt)$. Equation (32) shows that the slice picture developed on Fig 1 is still valid, except that slices located at X and $X+\pi$ are now coupled. The wave function can thus be written as

$$\psi_\beta(X+wt,t) = c_1(X,t)\psi_\beta(X,0) + c_2(X,t)\psi_\beta(X-\pi,0), \tag{33}$$

where c_1 and c_2 are 2π-periodic in X. For each X, the $c_j(X,t)$ $(j=1,2)$ define a "two-level" system, whose state can be written as the state vector

$$\mathbf{c}_t = \begin{pmatrix} c_1(X,t) \\ c_2(X-\pi,t) \end{pmatrix},$$

and whose recursion relation as a matrix relation

$$\mathbf{c}_t = \mathbf{M}_t\mathbf{c}_{t-1} = \prod_{s=0}^{t-1}\mathbf{M}_{t-s}\mathbf{c}_0 \tag{34}$$

where $\mathbf{M}_t$ is a 2×2 matrix given in Eq. (A.4) of Appendix A. In Ref. [1], we used this vector formailsm to calculate the mean momentum:

$$\langle P\rangle_\beta(t) = \langle P\rangle_\beta(t-1) + K\int_{-\pi}^{\pi} dX\sin(X+wt) \times\left(|c_1(X,t)|^2 - |c_2(X-\pi,t)|^2\right). \tag{35}$$

This means that the sub-packet at $X+wt$ receives a momentum equal to $K\sin(X+wt)$, and the one at $X+wt+\pi$ receives $-K\sin(X+wt)$, which is a straightforward genralization of the arguments developed in Sec. 2 for simple quantum resonances. The fundamental difference here is that the two sub-packets interfere during their free evolution, which does not allow any classical-like interpretation.

In the particular case $\beta = 0$, a fully analytical description can be made, which leads to the final expression for the mean momentum [1]

$$\langle P\rangle_{\beta=0}(t) = \langle P\rangle_{\beta=0}(t=0) + K\int_{-\pi}^{\pi} dX\,|c_1(X,0)|^2\sin X \times\left[\left(\frac{\sin^2\phi}{1+\sin^2\phi}\right)t + \frac{1}{1+\sin^2\phi}\left(\frac{\sin\left[(2t+1)\Theta\right]}{2\sin\Theta} - \frac{1}{2}\right)\right], \tag{36}$$

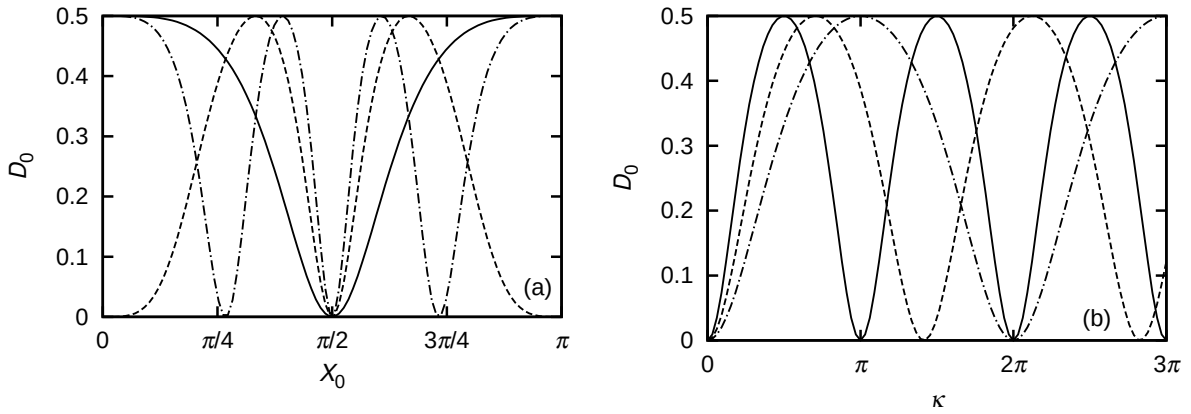

Figure 3. Factor D_0, reflecting the influence of interference effects on the ballistic rate for the QR at $\hbar = \pi$. On panel (a), D_0 is plotted as a function of X_0: for $\kappa = \pi/2$ (solid lines), $\kappa = \pi$ (dashed lines) and $\kappa = 3\pi/2$ (dashed-dotted lines). On panel (b), D_0 is plotted as a function of κ: for $X_0 = 0$ (solid lines), $X_0 = \pi/4$ (dashed lines) and $X_0 = \pi/3$ (dashed-dotted lines).

where $\phi = \phi(X, t = 0) = \kappa \cos X$, and Θ is such that

$$\cos \Theta = \frac{\cos \phi}{\sqrt{2}}. \tag{37}$$

The mean momentum exhibits more a complex behavior than for the SQRs. To analyze this result, we now consider an initial wavepacket localized at $X = X_0$. We see that the dynamics in general combines both oscillatory and ballistic behaviors. As time increases the ballistic part becomes dominant, and the momentum is approximately $\langle P \rangle_0 (t) \approx \langle P \rangle_0 (0) + D_2 t$, with the rate

$$D_2 = D_0 K \sin X_0, \tag{38}$$

where we set

$$D_0 = \frac{\sin^2 (\kappa \cos X_0)}{1 + \sin^2 (\kappa \cos X_0)}. \tag{39}$$

This diffusion rate is the one obtained for the SQRs, multiplied by a factor D_0 which reflects the interference effects. Figure 3 shows that this coefficient does not depend monotonously on κ. which is a direct consequence of the presence of quantum interferences. The diffusion rate can even totally vanish for particular values of κ and X_0. For example if $X_0 = \pi/2$, although the kicks communicate the maximum momentum to the wavepacket, the ballistic rate is strictly zero.

3.2. Mean kinetic energy

We now turn to the study of the effect of this interference on the average kinetic energy, with once again, a particular attention to the case $\beta = 0$.

3.2.1. The general case. We start from Eq. (B1) of [1]. We straightforwardly get to the relation

$$\langle E\rangle_\beta(t) = \langle E\rangle_\beta(t-1) + \frac{K^2}{2}\int_{-\pi}^{\pi} dX \sin^2(X+wt)\,|\psi_\beta(X+wt,t)|^2 + K\int_{-\pi}^{\pi} dX \sin\left(X+w(t-1)\right) J'(X+wt,t-1), \tag{40}$$

where, by analogy to Eq. (11), we defined the current

$$J'(X,t) = \frac{\hbar}{2} e^{i\beta\pi}\psi^*_\beta(X,t)\frac{\partial}{\partial X}\psi_\beta(X-\pi,t) + \text{c.c.} \tag{41}$$

As we did for the mean momentum, we express the mean kinetic energy in terms of the c_j functions. As shown in Appendix A, this implies that we also define the derivatives of the c_j functions with respect to X, that can also be written in a vector form

$$\mathbf{c'}_t = \begin{pmatrix} \frac{\partial}{\partial X}c_1(X,t) \\ \frac{\partial}{\partial X}c_2(X+\pi,t) \end{pmatrix} = \begin{pmatrix} c'_1(X,t) \\ c'_2(X+\pi,t) \end{pmatrix}. \tag{42}$$

It is shown in Appendix A that c'_t obeys the recursion relation

$$\mathbf{c'}_t = \mathbf{A}_t\mathbf{c}_t + e^{-i\frac{\pi}{4}}\mathbf{M}_t\mathbf{c'}_{t-1}, \tag{43}$$

where

$$\mathbf{A}_t = i\kappa\sin\left(X+wt\right)\begin{pmatrix} 1 & 0 \\ 0 & -1 \end{pmatrix}, \tag{44}$$

is diagonal and $\mathbf{M}_t$ (see Eq. (A.4)) is the matrix applied on vector $\mathbf{c}_t$. Iterating (43) down to $t=0$, we can write $\mathbf{c}'_t$ as a function of the initial conditions

$$\begin{aligned}
\mathbf{c'}_t &= \mathbf{A}_t\mathbf{c}_t + \mathbf{M}_t\left(\mathbf{A}_{t-1}\mathbf{c}_{t-1} + \mathbf{M}_{t-1}\left(\mathbf{A}_{t-2}\mathbf{c}_{t-2} + \ldots\right)\right) \\
&= \mathbf{A}_t\mathbf{c}_t + \mathbf{M}_t\mathbf{A}_{t-1}\mathbf{c}_{t-1} + \mathbf{M}_t\mathbf{M}_{t-1}\mathbf{A}_{t-2}\mathbf{c}_{t-2} + \ldots \\
&= \sum_{s=0}^{t-1}\left(\prod_{r=1}^{s}\mathbf{M}_{t-r}\right)\mathbf{A}_{t-s}\mathbf{c}_{t-s} \\
&= \left\{\sum_{s=0}^{t-1}\left(\prod_{r=1}^{s}\mathbf{M}_{t-r}\right)\mathbf{A}_{t-s}\left(\prod_{q=0}^{t-s-1}\mathbf{M}_{t-s-q}\right)\right\}\times\mathbf{c}_0.
\end{aligned} \tag{45}$$

We get a complex equation that is subtantially simpler in the particular case of $\beta = 0$.

3.2.2. The special case $\beta = 0$. In this particular case, $\mathbf{A}_t$ and $\mathbf{M}_t$ are time-independent. Therefore (45) becomes

$$\mathbf{c'}_t = \left(\sum_{s=0}^{t-1}\mathbf{M}_t^s\mathbf{A}_t\mathbf{M}_t^{t-s}\right)\times\mathbf{c}_0. \tag{46}$$

The main difficulty to calculate $\mathbf{c}'_t$ is that, unlike $\mathbf{A}_t$, $\mathbf{M}_t$ is not diagonal in the basis defined by the two levels of our system, denoted in what follows, as the physical basis. So, in order to calculate $\mathbf{M}_t^s$ and $\mathbf{M}_t^{t-s}$, we express $\mathbf{M}_t$ in its eigenbasis using Eq. (A.6). However, we need to go back to the physical basis to apply $\mathbf{A}_t$. In summary, starting from $\mathbf{c}_0$ in the physical basis, we must

- go to the eigenbasis of $\mathbf{M}_t$;
- apply $\mathbf{M}_t^{t-s}$ which is then diagonal;
- go back to the physical basis, and apply $\mathbf{A}_t$ which is diagonal;
- once again change basis, and apply $\mathbf{M}_t^s$;
- finally go back to the physical basis.

This operation is of course made for each value of s.

By doing so, and after cumbersome calculations we get to the expressions

$$\begin{aligned} c_1'(X,t) \quad &= i\kappa \sin X e^{-it\frac{\pi}{4}} \times \left[\frac{1}{2}\frac{\cos\Theta}{\sin^3\Theta}\sin(t\Theta)\right. \\ &\left. +t\left(\cos(t\Theta) - \frac{i}{\sqrt{2}}\frac{\sin\phi}{\sin\Theta}\sin(t\Theta)\right)\right] \qquad (47) \\ c_2'(X+\pi,t) &= i\kappa \sin X e^{-it\frac{\pi}{4}}\frac{e^{i\phi}}{\sin\Theta} \times \left[-\frac{1}{2}\frac{\sin\phi}{\sin\Theta}t\cos(t\Theta)\right. \\ &\left. +t\left(\frac{i}{2}\frac{\sin\phi\cos\Theta}{\sin^2\Theta} + \frac{i}{\sqrt{2}}\right)\sin(t\Theta)\right]. \qquad (48) \end{aligned}$$

We see that $c_1'(X,t)$ and $c_2'(X,t)$ are composed of oscillatory terms, some of them being multiplied to t. As will show the calculation of the mean kinetic energy, those unbounded terms are responsible for the ballistic behavior.

To calculate the mean kinetic energy, we have to apply our vector formalism to the general recursion equation (40). Once the integrals in (40) have been calculated (see Appendix B), we obtain the expression for an initial wavepacket localized around X_0

$$\begin{aligned} \langle E\rangle_{\beta=0}(t) = \langle E\rangle_{\beta=0}(t=0) + \frac{K^2}{2}\sin^2 X_0 \left\{\frac{\sin^2\phi}{1+\sin^2\phi}t^2\right. \\ + \frac{1}{4\sin^2\Theta}\left(\frac{1}{\sin^2\Theta} + \frac{\sin((2t-1)\Theta)}{\sin\Theta}\right. \\ \left.\left. -\frac{\cos\Theta}{\sin^2\Theta}\cos((2t-1)\Theta)\right)\right\}. \qquad (49) \end{aligned}$$

Once again, we find a combination of oscillatory and ballistic dynamics, whose rate can be written as

$$D' = \frac{K^2}{2}D_0 \sin^2 X', \qquad (50)$$

where D_0 is given by Eq. (39). This result for the diffusion rate has been found in Ref. [29], with a different method. Our result for kinetic energy is strongly similar to the one for momentum: the diffusion rate is that of RQS case, by multiplied by the interference factor D_0, which indicates how the two sub-packets have interfered with each other throughout the dynamical evolution.

3.3. Non-zero quasi-momenta

We have seen above that interference effects can be totally destructive reducing ballistic rate strictly to zero. We have also shown that anti-resonnant behavior leads to

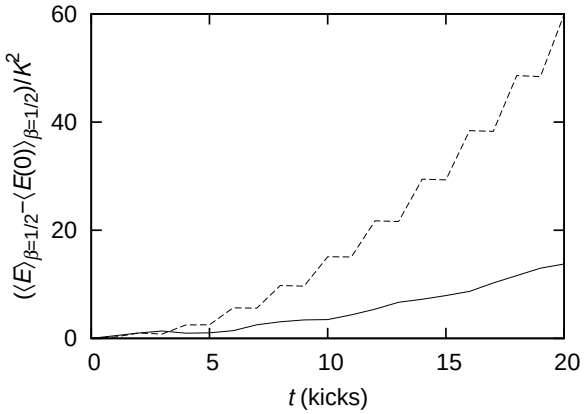

Figure 4. Combination of ballistic and oscillatory behaviors observed on the time evolution of the mean kinetic energy for $\hbar = \pi$ and $\beta = 1/2$. The initial state is a gaussian of momentum width $5/\sqrt{2}$ and centered at: $X = \pi/4$ (solid lines); $X = \pi/3$ (dashed lines), hence the different ballistic rates.

periodicity. Do such effects persist for non-zero quasi-momenta, and can they survive to averaging over β? Mathematically speaking, for $\beta = 0$, ballisticity is linked to the time-invariance of the $\mathbf{M}_t$ and $\mathbf{A}_t$ matrices. In the next paragraph, we will show that this time-independency can be found under some conditions for $\beta \neq 0$, namely $\beta = 1/2$. Next we will average over quasi-momenta.

If $\beta = 1/2$ ($w = \pi/2$), the two sub-packets will come back to their initial positions after 4 kicks, the dynamics is thus described by a matrix

$$\mathbf{M}' = \mathbf{M}_4\mathbf{M}_3\mathbf{M}_2\mathbf{M}_1 \tag{51}$$

which is time-independent. Therefore, a similar work can be performed with $\mathbf{M}'$ as the one done with $\mathbf{M}$ with $\beta = 0$. We can expect the same qualitative results for the dynamical behavior, i.e. a combination of balistic and oscillatory behaviors. Fig. 4 shows numerical results giving the time evolution of the kinetic energy which is good agreement with our arguments. However since $\mathbf{M}'$ covers a 4-kick period, we can roughly estimate the ballistic rate as 4 times smaller. More generally, we can expect that ballisticity emerges for any rational quasimomentum p/q, but a rate scaling as $1/q$. In the limit $q \to \infty$, i.e. irrational quasimomentum, ballisticity disappears.

These arguments are partly confirmed by the numerical simulations shown on Fig. 5. We calculation the mean kinetic energy after 80 kicks as a function of β. To get rid of the X dependence of ballisticity (see Eq. (39)), the initial conditions are plane waves of momentum $\hbar\beta$. We clearly see ballistic peaks, the highest of which correspond to the "most rational" quasi-momenta. Note however some differences with the arguments above: for example the energy is higher for $\beta = 1/2$ than for $\beta = 0$. This is because the value of $K = 10$ induces rather destructive interferences for certain quasi-momenta and rather constructive ones for other β. A different value of K would modify this balance.

Fig. 6 concerns the behavior of the average kinetic energy corresponding to an initial momentum distribution which is a few times the Brillouin zone, and shows

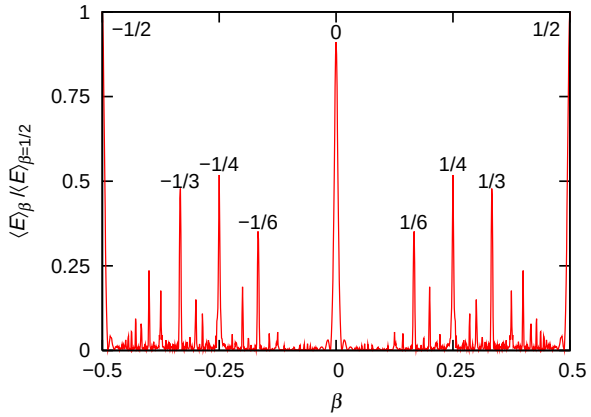

Figure 5. Mean kinetic energy plotted as a function of β after 80 kicks for $\hbar = \pi$. For each quasimomentum the initial state is a plane wave whose mean momentum is $\hbar\beta$. The peaks corresponding to ballistic dynamics arise for rational quasi-momenta. The highest ones are indexed. $K = 10$.

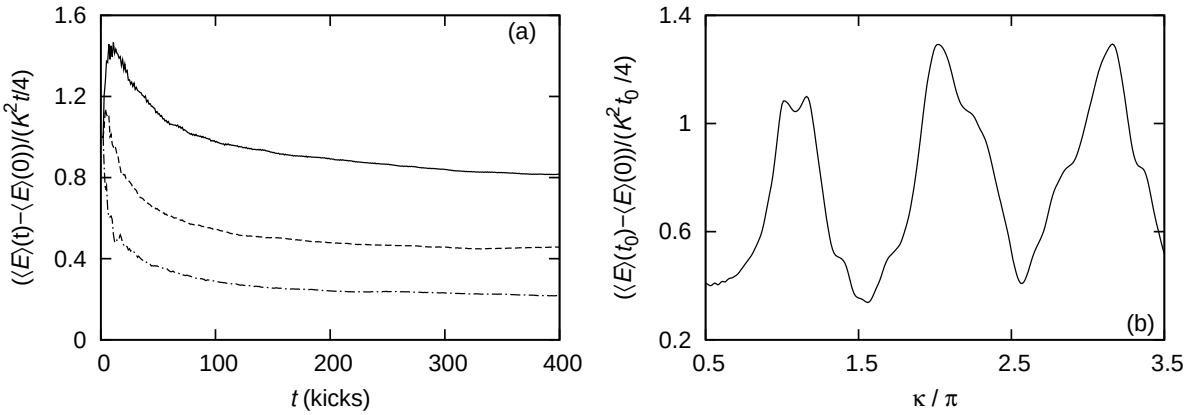

Figure 6. Interference effects resulting in the oscillatory dependence on K of the mean kinetic energy in the $\hbar = \pi$. On panel (a), $\langle E\rangle$ is plotted as a function of time for different values of the kicking strength: solid lines for $K = 1,1\pi^2$ ($\kappa = 1,1\pi$); dashed lines for $K = 1,3\pi^2$ ($\kappa = 1,3\pi$); dashes-dotted lines $K = 1,5\pi^2$ ($\kappa = 1,5\pi$). On panel (b), $\langle E\rangle$ is plotted as a function of κ after $t_0 = 60$ kicks. The initial momentum distribution is "broad", i.e. a gaussian of width $5/\sqrt{2}$; to mimick an (incoherent) atomic cloud each quasimomentum is given a random phase.

essentially a diffusive behavior. Clearly, although it concerns a higher number of quasi-momenta, ballisticity does not survive the averaging process. The diffusion rate presents an oscillatory behavior as a function of κ, but never goes to zero: quantum interferences survive when averaging over a broadband initial momentum distribution, but with a reduced contrast.

4. Conclusion

In this paper, we have extended the analysis of quantum resonances given in [1] to systems of experimental interest, characterized by strongly delocalized wave functions in position space. We have extensively used the ideas presented in our preceding work to interpret our present results.

In the case of simple quantum resonances, we have made an analytical treatment based on the map giving the mean position and momentum. We have considered two examples of initial momentum distributions. For a narrow distribution, we have seen that the behavior of the central quasi-momentum persists for a time proportional to the inverse distribution width. We have demonstrated that the ballistic motion is progressively replaced by a diffusive regime, whose rate is also proportional to the inverse distribution width. In the anti-resonant case, we have shown that the oscillations of the average kinetic energy are progressively damped, until the dynamics becomes "frozen" in momentum space. Strikingly, we have found that the form of the damping keeps the track of the initial momentum distribution. We have also explained the diffusive behavior observed with broad initial distribution, which is a consequence of the dispersion of the momenta communicated to the atom by each kick. In the $\hbar = \pi$ high-order resonance, we have extended our previous calculations to the average kinetic energy and shown that interference effects persist even for a broad initial momentum distribution.

An interesting prospect of the present work is its application to the case where interactions between atoms are present (e.g. one uses a dense Bose-Einstein codensate). A first experimental study of such a system has been made by Raizen and co-workers [30], and it was demonstrated in [24] that for a weak interaction strength, the resonant value of $\hbar$ is shifted. Moreover the latter work shows that the diffusion coefficient presents sharp edges as the nonlinearity is varied, which are still unexplained. A kind of nonlinear *optical* Talbot effect has been observed recently in an optical system [31], which hints that our approach could be generalized to this much more complex case.

Appendix A. Vector formalism and mean kinetic energy

In this appendix, we want to apply the vector formailsm defined in Ref. [1] for $\hbar = \pi$, to the calculation of the mean kinetic energy (see Eq. (32)). To that goal, we derive Eq. (33) with respect to X to get $\frac{\partial \psi_\beta}{\partial X}$

$$\begin{aligned}\frac{\partial}{\partial X}\psi_\beta(X+wt,t) = \frac{\partial}{\partial X}c_1(X,t)\psi_\beta(X,0) + c_1(X,t)\frac{\partial}{\partial X}\psi_\beta(X,0). \\ + \frac{\partial}{\partial X}c_2(X,t)\psi_\beta(X-\pi,0) \\ + c_2(X,t)\frac{\partial}{\partial X}\psi_\beta(X-\pi,0). \end{aligned} \tag{A.1}$$

This equation contains the derivative of the c_j functions, whose recursion realation is straightforwardly found by deriving (A.4):

$$\begin{aligned}\frac{\partial}{\partial X}c_1(X,t) \quad &= i\kappa \sin\left(X+wt\right) c_1(X,t) \\ &+ \frac{e^{-i\phi(X,t)}}{\sqrt{2}}\left[e^{-i\pi/4}\frac{\partial}{\partial X}c_1(X,t-1)\right. \\ &\left. +e^{i\pi/4}e^{-i\beta\pi}\frac{\partial}{\partial X}c_2(X+\pi,t-1)\right] \qquad \text{(A.2)} \\ \frac{\partial}{\partial X}c_2(X+\pi,t) = &-i\kappa \sin\left(X+wt\right) c_2(X+\pi,t) \\ &+ \frac{e^{i\phi(X,t)}}{\sqrt{2}}\left[e^{i\pi/4}e^{i\beta\pi}\frac{\partial}{\partial X}c_1(X,t-1)\right. \\ &\left. +e^{-i\pi/4}\frac{\partial}{\partial X}c_2(X+\pi,t-1)\right]. \qquad \text{(A.3)}\end{aligned}$$

Finally by setting $t=0$ and identifying the two sides of Eq. (A.1), we get the initial conditions

$$\begin{aligned}&\frac{\partial}{\partial X}c_1(X,t=0)=0 \\ &\frac{\partial}{\partial X}c_2(X,t=0)=0.\end{aligned}$$

One important property of the $\frac{\partial c_j}{\partial X}$, which can be seen by applying Eqs. (A.2) and (A.3) recursively, is their 2π-periodicity.

By writing the $\frac{\partial c_j}{\partial X}$ functions in a vector form (see Eq. (42)), we get to the recursion (43), with

$$\mathbf{M}_t = \frac{e^{-i\pi/4}}{\sqrt{2}}\begin{pmatrix} e^{-i\phi} & ie^{-i\phi}e^{-i\beta\pi} \\ ie^{i\phi}e^{i\beta\pi} & e^{i\phi}\end{pmatrix}, \qquad \text{(A.4)}$$

and the initial condition

$$\mathbf{c}_0 = \begin{pmatrix}1\\0\end{pmatrix}. \qquad \text{(A.5)}$$

We recall form Ref. [1] that, for $\beta=0$, $\mathbf{M}_t$ is time-independent. Therefore $\mathbf{c}_t$ can be written as

$$\mathbf{c}_t = e^{-it\frac{\pi}{4}}\mathbf{P}\begin{pmatrix} e^{it\Theta} & 0 \\ 0 & e^{-it\Theta}\end{pmatrix}\mathbf{P}^{-1}\mathbf{c}_0, \qquad \text{(A.6)}$$

where $\exp\left(\pm i\Theta\right)$ are the eigenvalues of $\mathbf{M}_t$, with Θ given by $\cos\Theta = \frac{\cos(\kappa\cos X)}{\sqrt{2}}$, and $\mathbf{P}$ is the diagonalization matrix

$$\mathbf{P} = \begin{bmatrix} -ie^{-i\phi} & -ie^{-i\phi} \\ e^{-i\phi}-\sqrt{2}e^{i\Theta} & e^{-i\phi}-\sqrt{2}e^{-i\Theta}\end{bmatrix}. \qquad \text{(A.7)}$$

Those relations are of a great interest to establish Eq. (43).

Appendix B. Mean kinetic energy for $\beta = 0$

The goal of this appendix is to show how to apply our vector formalism to derive a recursion relation on mean kinetic energy for $\beta = 0$. Starting from Eq. (40) and replacing the wave function $\psi_\beta(X,t)$ and its derivative by their two-level expensions (33) and (A.1), we have to calculate the two integrals in (40), which is done by using the assumption that $\psi_\beta(X,0)$ and $\frac{\partial}{\partial X}\psi_\beta(X,0)$ is much more localized around $X = X_0$ than any other function envolved in these integrals.

Therefore, the integral in $\sin^2$ yields

$$\begin{aligned}
&\frac{K^2}{2}\int_{-\pi}^{\pi} dX \sin^2 X \left|\psi_\beta(X,t)\right|^2 \\
&= \frac{K^2}{2}\int_{-\pi}^{\pi} dX \sin^2\left(X_0 + wt\right)\left|\psi_\beta(X,0)\right|^2 \\
&\quad \times \left(\left|c_1(X,t)\right|^2 + \left|c_2(X+\pi,t)\right|^2\right) \\
&= \frac{K^2}{2}\sin^2\left(X_0 + wt\right), \qquad \text{(B.1)}
\end{aligned}$$

where we used the normalization property $|c_1(X,t)|^2 + |c_2(X+\pi,t)|^2 = 1, \forall X$. As for the J' term, it reads

$$\begin{aligned}
&K\int_{-\pi}^{\pi} dX \sin X J'(X - w, t-1) \\
&= \frac{\hbar K}{2} e^{i\beta\pi}\int_{-\pi}^{\pi} dX \sin\left(X + w\left(t-1\right)\right) \\
&\times \left(c_1^*\left(X\right)\psi_\beta^*\left(X\right) + c_2^*\left(X\right)\psi_\beta^*\left(X-\pi\right)\right) \\
&\times \Big(c_1'\left(X-\pi\right)\psi_\beta\left(X-\pi\right) + c_1\left(X-\pi\right)\psi_\beta'\left(X-\pi\right) \\
&\quad + c_2'\left(X-\pi\right)\psi_\beta\left(X-2\pi\right) + c_2\left(X-\pi\right)\psi_\beta'\left(X-2\pi\right)\Big) + cc \\
&= \frac{\hbar K}{2} e^{i\beta\pi}\int_{-\pi}^{\pi} dX \sin\left(X + w\left(t-1\right)\right) \\
&\times \Big(e^{-i2\pi\beta} c_1^*\left(X\right) c_2'\left(X-\pi\right)\left|\psi_\beta\left(X\right)\right|^2 \\
&\quad + c_2^*\left(X\right) c_1'\left(X-\pi\right)\left|\psi_\beta\left(X-\pi\right)\right|^2 \\
&\quad + e^{-i2\pi\beta} c_1^*\left(X\right) c_2\left(X-\pi\right)\psi_\beta^*\left(X\right)\psi_\beta'\left(X\right) \\
&\quad + c_2^*\left(X\right) c_1\left(X-\pi\right)\psi_\beta^*\left(X-\pi\right)\psi_\beta'\left(X-\pi\right)\Big) + cc., \qquad \text{(B.2)}
\end{aligned}$$

where for the sake of clarity, we removed all the time-dependences. Integrating over X gives

$$\begin{aligned}
&K\int_{-\pi}^{\pi} dX \sin X J'(X - w, t-1) \\
&= \frac{\hbar K}{2}\sin\left(X_0 + w\left(t-1\right)\right) \\
&\quad \times \left(e^{-i\pi\beta} c_1^*\left(X'\right) c_2'\left(X_0+\pi\right) - e^{i\pi\beta} c_2^*\left(X_0+\pi\right) c_1'\left(X_0\right) + cc\right) \\
&+ iK\sin\left(X_0 + w\left(t-1\right)\right)\left\langle P\right\rangle_\beta\left(t=0\right) \\
&\quad \times \left(e^{-i\pi\beta} c_1^*\left(X_0\right) c_2\left(X_0+\pi\right) - e^{i\pi\beta} c_2^*\left(X_0+\pi\right) c_1\left(X_0\right)\right). \qquad \text{(B.3)}
\end{aligned}$$

As $\langle P\rangle_{\beta=0}(t=0)$ is zero, we get for the mean kinetic energy

$$\begin{aligned}\langle E\rangle_{\beta=0}(t) &= \langle E\rangle_{\beta=0}(t-1) + \frac{K^2}{2}\sin^2 X_0 + \hbar K \sin X_0 \\ &\quad \times \left(c_1^*(X_0)\, c_2'(X_0+\pi) - c_2^*(X_0+\pi)\, c_1'(X_0) + cc\right). \end{aligned} \tag{B.4}$$

Finally replacing c_1, c_2, c_1' and c_2' by their respective expressions yields

$$\begin{aligned}\langle E\rangle_{\beta=0}(t) &= \langle E\rangle_{\beta=0}(t-1) + \frac{K^2}{2}\sin^2 X_0 \\ &\quad \times \left\{ \frac{\sin^2\phi}{1+\sin^2\phi}(2t-1) + \frac{1}{1+\sin^2\phi} \right. \\ &\quad \left. \times \left(\cos\left((2t-2)\,\Theta\right) + \frac{\cos\Theta}{\sin\Theta}\sin\left((2t-2)\,\Theta\right)\right)\right\}. \end{aligned} \tag{B.5}$$

By iteraing down to $t=0$, we get to Eq. (49).

References

[1] M. Lepers, V. Zehnlé, and J. C. Garreau. Kicked-rotor quantum resonances in position space. *Phys. Rev. A*, 77(4):043628, 2008.

[2] H. J. Stökmann. *Quantum Chaos an Introduction*. Cambridge University Press, Cambridge, UK, 1999.

[3] M. C. Gutzwiller. *Chaos in Classical and Quantum Mechanics*. Springer-Verlag, Berlin, Germany, 1986.

[4] A. J. Lichtenberg and M. A. Lieberman. *Regular and Chaotic Dynamics*. Springer-Verlag, Berlin, Germany, 1982.

[5] F. L. Moore, J. C. Robinson, C. F. Bharucha, B. Sundaram, and M. G. Raizen. Atom Optics Realization of the Quantum δ-Kicked Rotor. *Phys. Rev. Lett.*, 75(25):4598–4601, 1995.

[6] H. Ammann, R. Gray, I. Shvarchuck, and N. Christensen. Quantum Delta-kicked rotator: experimental observation of decoherence. *Phys. Rev. Lett.*, 80:4111–4115, 1998.

[7] B. G. Klappauf, W. H. Oskay, D. A. Steck, and M. G. Raizen. Experimental Study of Quantum Dynamics in a Regime of Classical Anomalous Diffusion. *Phys. Rev. Lett.*, 81(19):4044–4047, 1998.

[8] M. K. Oberthaler, R. M. Godun, M. B. d'Arcy, G. S. Summy, and K. Burnett. Observation of quantum accelerated modes. *Phys. Rev. Lett.*, 83(22):4447–4451, 1999.

[9] J. Ringot, P. Szriftgiser, J. C. Garreau, and D. Delande. Experimental Evidence of Dynamical Localization and Delocalization in a Quasiperiodic Driven System. *Phys. Rev. Lett.*, 85(13):2741–2744, 2000.

[10] P. H. Jones, M. M. Stocklin, G. Hur, and T. S. Monteiro. Atoms in Double-δ-Kicked Periodic Potentials: Chaos with Long-Range Correlations. *Phys. Rev. Lett.*, 93(22):223002, 2004.

[11] P. H. Jones, M. Goonasekera, and F. Renzoni. Rectifying Fluctuations in an Optical Lattice. *Phys. Rev. Lett.*, 93(7):073904, 2004.

[12] H. Lignier, J. Chabé, D. Delande, J. C. Garreau, and P. Szriftgiser. Reversible Destruction of Dynamical Localization. *Phys. Rev. Lett.*, 95(23):234101, 2005.

[13] J. Chabé, H. Lignier, H. Cavalcante, D. Delande, P. Szriftgiser, and J. C. Garreau. Quantum Scaling Laws in the Onset of Dynamical Delocalization. *Phys. Rev. Lett.*, 97(26):264101, 2006.

[14] J. Chabé, G. Lemarié, B. Grémaud, D. Delande, P. Szriftgiser, and J. C. Garreau. Experimental Observation of the Anderson Metal-Insulator Transition with Atomic Matter Waves. *Phys. Rev. Lett.*, 101(25):255702, 2008.

[15] I. Dana, V. Ramareddy, I. Talukdar, and G. S. Summy. Experimental Realization of Quantum-Resonance Ratchets at Arbitrary Quasimomenta. *Phys. Rev. Lett.*, 100(2):024103, 2008.

[16] Z. Y. Ma, M. B. d'Arcy, and S. A. Gardiner. Gravity-Sensitive Quantum Dynamics in Cold Atoms. *Phys. Rev. Lett.*, 93(16):164101, 2004.

[17] G. Lemarié, J. Chabé, P. Szriftgiser, J. C. Garreau, B. Grémaud, and D. Delande. Observation of the Anderson metal-insulator transition with atomic matter waves: Theory and experiment. *Phys. Rev. A*, 80(4):043626, 2009.

[18] G. Lemarié, H. Lignier, D. Delande, P. Szriftgiser, and J. C. Garreau. Critical State of the Anderson Transition: Between a Metal and an Insulator. *Phys. Rev. Lett.*, 105(9):090601, 2010.

[19] S. Fishman, I. Guarneri, and L. Rebuzzini. Stable Quantum Resonances in Atom Optics. *Phys. Rev. Lett.*, 89(8):084101, 2002.

[20] S. Schlunk, M. B. d'Arcy, S. A. Gardiner, and G. S. Summy. Experimental Observation of High-Order Quantum Accelerator Modes. *Phys. Rev. Lett.*, 90(12):124102, 2003.

[21] S. Wimberger, M. Sadgrove, S. Parkins, and R. Leonhardt. Experimental verification of a one-parameter scaling law for the quantum and "classical" resonances of the atom-optics kicked rotor. *Phys. Rev. A*, 71(5):053404, 2005.

[22] G. Behinaein, V. Ramareddy, P. Ahmadi, and G. S. Summy. Exploring the Phase Space of the Quantum delta-Kicked Accelerator. *Phys. Rev. Lett.*, 97(24):244101, 2006.

[23] S. Wimberger, I. Guarneri, and S. Fishman. Quantum resonances and decoherence for δ-kicked atoms. *Nonlinearity*, 16(4):1381–1420, 2003.

[24] T. S. Monteiro, A. Ranon, and J. Ruostekoski. Nonlinear Resonances in delta-Kicked Bose-Einstein Condensates. *Phys. Rev. Lett.*, 102(1):014102, 2009.

[25] V. Ramareddy, G. Behinaein, I. Talukdar, P. Ahmadi, and G. S. Summy. High-order resonances of the quantum δ-kicked accelerator. *Europhys. Lett.*, 89(3):33001, 2010.

[26] M. V. Berry and E. Bodenchatz. Caustics, mutilply reconstructed by Talbot interference. *J. Mod. Opt.*, 46(2):349–365, 1999.

[27] F. M. Izrailev and D. L. Shepelyansky. Quantum resonance for a rotator in a nonlinear periodic field. *Th. Math. Phys.*, 43(3):553–561, 1980.

[28] B. V. Chirikov. A universal instability of many-dimensional oscillator systems. *Phys. Rep.*, 52(5):263–379, 1979.

[29] V. V. Sokolov, O. V. Zhirov, D. Alonso, and G. Casati. Quantum resonances and regularity islands in quantum maps. *Phys. Rev. E*, 61(5):5057–5072, 2000.

[30] K. Henderson, H. Kelkar, B. Gutiérrez-Medina, T. C. Li, and M. G. Raizen. Experimental Study of the Role of Atomic Interactions on Quantum Transport. *Phys. Rev. Lett.*, 96(15):150401, 2006.

[31] Y. Zhang, J. Wen, S. N. Zhu, and M. Xiao. Nonlinear Talbot Effect. *Phys. Rev. Lett.*, 104(18):183901, 2010.